Inorg. Chem. **1990**, *29*, 1784-1787

4905 cm^{-1} for an intervalence charge-transfer (IT) transition.[12] Cyclic voltammetry of **1** in CH_2Cl_2–TBAP at 5 °C showed two oxidations and one reduction processes that are believed to be metal centered with the following $E_{1/2}$, V vs SCE (ΔE_p, mV) values: +0.615 (130), +0.230 (120), and −0.435 (150), respectively, at 20 mV s^{-1}. A peak at δ 16.98 in the ^{1}H NMR spectra of **1** in $CDCl_3$ is assignable to a μ-OH_2 group.

The X-ray structure of **1** is shown in Figure 2.[13] The molecule consists of a diruthenium(III,II) unit held by an aqua bridge and two bridging carboxylato ligands forming an $\{Ru_2(\mu\text{-}OH_2)(\mu\text{-}O_2CAr)_2{}^{3+}\}$ core. In this asymmetric molecule the metal centers are clearly distinguishable. The oxidation states of Ru(1) and Ru(2) are +2 and +3, respectively, since the Ru(1)–O(1) distance of 2.143 (12) Å is considerably longer than the Ru(2)–O(1) bond length of 2.107 (10) Å. Compound **1** thus exemplifies a trapped mixed-valence system.

The formal identification of a μ-OH_2 bridge in **1** is based on the location of two hydrogen atoms. The presence of strong hydrogen bonds is also inferred from the short O(1)···O(12) and O(1)···O(31) distances.[14] The considerably different O(1)–H(1) and O(1)–H(2) bond lengths could be due to the thermally unstable nature of **1**.

The unusual structural feature in **1** is the presence of three different types of ligands on the facial sites of each ruthenium. In the formation of **1**, the polymeric network of $[Ru_2Cl(\mu\text{-}O_2CAr)_4]_x$ is cleaved into discrete dimeric units along with a segregation of the oxidation states to $Ru^{III}Ru^{II}$ from the $Ru_2{}^{5+}$ core in the $\sigma^2\ \pi^4\ \delta^2\ (\delta^*\ \pi^*)^3$ ground electronic configuration of the starting compound. The Ru(1)–Ru(2) distance of 3.605 (2) Å in **1** is quite long for any direct Ru–Ru bond formation.

Compound **1** is unstable in the solution phase. In $CHCl_3$, it slowly forms a purple compound, $[\{Ru(PPh_3)(O_2CAr)\}_2(\mu\text{-}O)(\mu\text{-}O_2CAr)_2]$ (**3**), while in MeCN it converts to a blue species, $[\{Ru(PPh_3)(MeCN)_2\}_2(\mu\text{-}O)(\mu\text{-}O_2CAr)_2](ClO_4)_2$ (**4**), isolated as a perchlorate salt. Molecular structures of **3** and **4**, determined by X-ray studies,[15] show the presence of an $\{Ru_2(\mu\text{-}O)(\mu\text{-}O_2CAr)_2{}^{2+}\}$ met-analogue[4] core in these diamagnetic diruthenium(III) complexes. The facile formations of **3** and **4** are believed to be redox controlled, associated with ligand substitution.

Acknowledgment. This work is supported by the CSIR, New Dehli. We thank Professor H. Manohar and I. I. Mathews for their help in the X-ray structural studies.

Supplementary Material Available: Tables I–IV, listing atomic coordinates, bond lengths, bond angles, and thermal parameters (13 pages); Table V, listing observed and calculated structure factors for **1** (23 pages). Ordering information is given on any current masthead page.

---

(12) (a) Creutz, C. *Prog. Inorg. Chem.* **1983**, *30*, 1. (b) Richardson, D. E.; Taube, H. *Coord. Chem. Rev.* **1984**, *60*, 107.

(13) X-ray analysis of **1**: Triclinic, $P\bar{1}$, a = 13.538 (5) Å, b = 15.650 (4) Å, c = 18.287 (7) Å, α = 101.39 (3)°, β = 105.99 (4)°, γ = 97.94 (3)°, V = 3574 Å^3, Z = 2, d(calcd) = 1.32 g cm^{-3}, d(obsd) = 1.34 g cm^{-3}, μ(Mo Kα) = 4.55 cm^{-1}, $F(000)$ = 1446. A total number of 12395 unique reflections were collected in the $4° \leqslant 2\theta \leqslant 50°$ range. R = 0.085 (unit weight) with 4092 reflections having $F_o > 10\sigma(F_o)$. Number of parameters = 474. Overall scale factor = 1.55. Largest shift/esd = 0.066. Highest peak in the final difference Fourier map = 1.12 e Å^{-3} at 1.18 Å from Ru(2). One of the arene groups of the bridging carboxylato ligands was found to be disordered, and these atoms were refined with a site occupancy of 0.5. The higher R factor is due to the unstable nature of the crystal (decay ca. 40%) during data collection, and the molecule is found to be disordered.

(14) Turpeinen, U.; Hämäläinen, R.; Reedijk, J. *Polyhedron* **1987**, *6*, 1603.

(15) Structural data on **3** with Ar = C_6H_4-p-OMe: Ru···Ru, Ru–(μ-O), and Ru–(μ-O)–Ru are 3.199 (3) Å, 1.860 (4) Å, and 118.7 (2)°, respectively. R = 0.065. Data for **4** with Ar = Ph: Ru···Ru, Ru–(μ-O), and Ru–(μ-O)–Ru are 3.240 (3) Å, 1.873 (4) Å, and 119.7 (2)°, respectively. R = 0.079. A detailed report on **3** and **4** will be made elsewhere.

Department of Inorganic and
Physical Chemistry
Indian Institute of Science
Bangalore 560 012, India

Birinchi K. Das
Akhil R. Chakravarty*

Received September 6, 1989

Polyoxoanions as Soluble Metal Oxide Analogues. 5.[1] Synthesis and Characterization of Polyoxoanion-Supported, Atomically Dispersed Iridium(I), $(1,5\text{-}COD)Ir\cdot P_2W_{15}Nb_3O_{62}{}^{8-}$

Polyoxoanions[1,2] are soluble oxides that resemble discrete fragments of solid metal oxides.[2c] As such, they are of considerable interest as catalyst support[3,4] materials, for both fundamental and practical reasons. However, a prototype catalyst precursor that leads to a polyoxoanion-*supported*[3] catalyst has not been previously described,[5] despite numerous reports over the last nine years of polyoxoanion-supported organometallics.[1,6] Herein we report the synthesis and characterization of $(Bu_4N)_5Na_3[(1,5\text{-}COD)Ir\cdot P_2W_{15}Nb_3O_{62}]$ (**1**) (Figure 3), which serves as an excellent precursor to an active and long-lived hydrogenation catalyst.[4] We also report key considerations and decision points that led to the successful combination of polyoxoanion (the second generation system,[1d] $P_2W_{15}Nb_3O_{62}{}^{9-}$), metal (Ir), coordinated ligand (1,5-COD), and counterions $[(Bu_4N)_5Na_3]$ in **1**, the *best* catalyst precursor from a series that we have prepared and examined.[7,8]

---

(1) Earlier Oregon work focused toward polyoxoanion-supported catalysts: (a) Finke, R. G.; Droege, M. W. *J. Am. Chem. Soc.* **1984**, *106*, 7274. (b) Finke, R. G.; Rapko, B.; Saxton, R. J.; Domaille, P. J. *J. Am. Chem. Soc.* **1986**, *108*, 2947. (c) Finke, R. G.; Rapko, B.; Domaille, P. J. *Organometallics* **1986**, *5*, 175. (d) Edlund, D. J.; Saxton, R. J.; Lyon, D. K.; Finke, R. G. *Organometallics* **1988**, *7*, 1692. See footnote 8a for a discussion of the challenges, and possible ion-pairing effects, presented by the presence of multiple cations like Bu_4N^+ and Na^+. (e) Supported $M(CO)_3{}^+$ monocations, specifically $(Bu_4N)_7[(OC)_3Re\cdot SiW_9Nb_3O_{40}]$[1f] and $(Bu_4N)_7[(OC)_3Re\cdot SiW_9V_3O_{40}]$,[1g] exhibit ^{183}W NMR spectra with poor S/N and multiple lines indicative of the presence of more than one isomer. On the other hand, for example, the single C_s symmetry isomer of $[(C_5Me_5)Rh\cdot SiW_9Nb_3O_{40}]^{5-}$ gives the expected high S/N, five-line ^{183}W NMR spectrum.[1a,c] (f) Droege, M. W. Ph.D. Dissertation, University of Oregon, 1984, p 196. (g) Rapko, B. Ph.D. Dissertation, University of Oregon, 1986, p 213. (h) Finke, R. G.; Lyon, D. K.; Nomiya, K.; Weakley, T. R. J. *Acta Crystallogr.*, in press.

(2) (a) Pope, M. T. *Heteropoly and Isopoly Oxometalates*; Springer-Verlag: New York, 1983. (b) Day, V. W.; Klemperer, W. G. *Science* **1985**, *228*, 533. (c) Baker, L. C. In *Advances in the Chemistry of the Coordination Compounds*; Kirschner, S., Ed.; MacMillian: New York, 1961; p 604.

(3) For a definition of polyoxoanion-*supported* metals, and their distinction from other bonding situations (e.g. polyoxoanion-*framework-incorporated* metals), see ref 1c, footnote 1f.

(4) Lyon, D. K.; Finke, R. G. *Inorg. Chem.*, following communication in this issue.

(5) (a) While reports have appeared[5b–e] of catalysis by mixtures containing certain types of polyoxoanions and organotransition-metal complexes, in each case the active catalyst, although quite interesting, is not a tightly supported transition-metal–polyoxoanion complex, either by design or due to the use of polyoxoanions with negligible or insufficient[5c] surface-oxygen charge density. (b) Urabe, K.; Tanaka, Y.; Izumi, Y. *Chem. Lett.* **1985**, 1595. (c) Che, T. M. U.S. Patent 4,590,298 assigned to Celanese Corp., May 20, 1986. (d) Siedle, A. R.; Markell, C. G.; Lyon, P. A.; Hodgson, K. O.; Roe, A. L. *Inorg. Chem.* **1987**, *26*, 219. (e) Siedle, A. R.; Newmark, R. A.; Gleason, W. B.; Skarjune, R. P.; Hodgson, K. O.; Roe, A. L.; Day, V. W. *Solid State Ionics* **1988**, *26*, 109.

(6) Studies by Klemperer, Day, and co-workers on the synthesis and structural characterization of polyoxoanion–organometallic complexes: (a) Besecker, C. J.; Klemperer, W. G. *J. Am. Chem. Soc.* **1980**, *102*, 7258. (b) Besecker, C. J.; Klemperer, W. G. *J. Organomet. Chem.* **1981**, *205*, C31. (c) Day, V. W.; Fredrich, M. F.; Thompson, M. R.; Klemperer, W. G.; Liu, R.-S.; Shum, W. *J. Am. Chem. Soc.* **1981**, *103*, 3597. (d) Besecker, C. J.; Klemperer, W. G.; Day, V. W. *J. Am. Chem. Soc.* **1982**, *104*, 6158. (e) Besecker, C. J.; Day, V. W.; Klemperer, W. G.; Thompson, M. R. *J. Am. Chem. Soc.* **1984**, *106*, 4125. (f) Besecker, C. J.; Day, V. W.; Klemperer, W. G.; Thompson, M. R. *Inorg. Chem.* **1985**, *24*, 44. (g) Besecker, C. J.; Day, V. W.; Klemperer, W. G. *Organometallics* **1985**, *4*, 564. (h) Day, V. W.; Klemperer, W. G.; Maltbie, D. J. *Organometallics* **1985**, *4*, 104.

(7) (a) Finke, R. G. Presented at the U.S.-Japan Seminar on the Catalytic Activity of Polyoxoanions, Shimoda, Japan, May 28–30, 1985 (preliminary studies of $(Bu_4N)_8[(1,5\text{-}COD)Rh\cdot P_2W_{15}Nb_3O_{62}]$ as an olefin hydrogenation precatalyst). (b) Finke, R. G. Presented at the 3rd Chemical Congress of the North American Continent, Symposium on Heteropoly Oxometalates, Toronto, Ontario, Canada, June 5–11, 1988 (studies of $(Bu_4N)_6[(1,5\text{-}COD)Ir\cdot SiW_9Nb_3O_{40}]$ and $(Bu_4N)_8[(1,5\text{-}COD)Ir\cdot P_2W_{15}Nb_3O_{62}])$. (c) Lyon, D. K. Presented at the 44th Northwest Regional Meeting of the American Chemical Society, Reno-Sparks, NV, June 1989; paper 127 (studies of $(Bu_4N)_5Na_3[(1,5\text{-}COD)Ir\cdot P_2W_{15}Nb_3O_{62}])$.

0020-1669/90/1329-1784$02.50/0

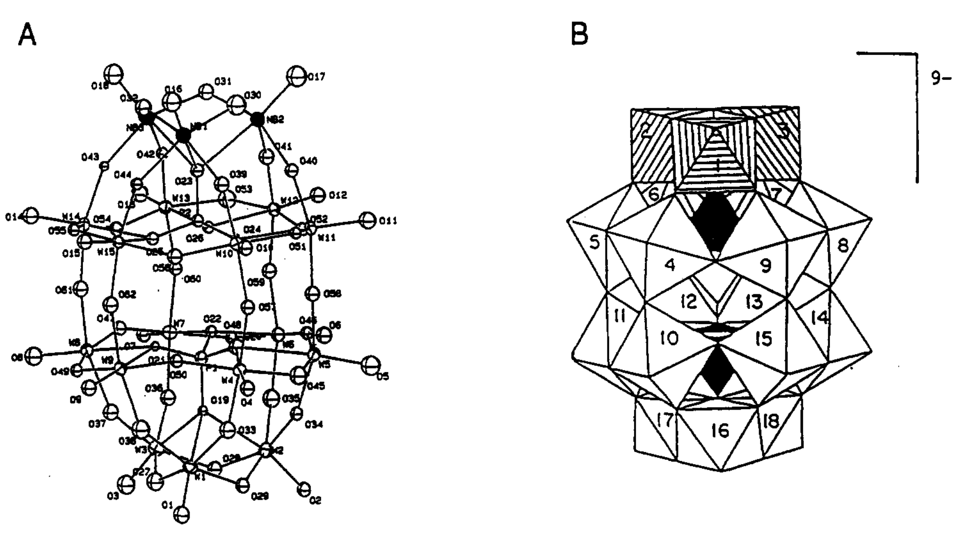

Figure 1. (A) Ball and stick representation of α-1,2,3-$P_2W_{15}Nb_3O_{62}^{9-}$ as determined by a single-crystal X-ray diffraction structural analysis.[2h] (For a discussion of the α structural descriptor, see ref 2c.) The darkened circles show the position of the three Nb atoms. (B) Polyhedral representation of α-1,2,3-$P_2W_{15}Nb_3O_{62}^{9-}$. The three niobiums are represented by the hatched octahedra in the 1–3-positions. The WO_6 octahedra occupy the 4–18-positions, and the PO_4 are shown as the two internal, black tetrahedra.

Our approach began from the key conceptual point that catalysis is a wholly kinetic phenomenon,[9] accomplished by intermediates and other transients but not generally by isolable complexes. Hence, our studies necessarily started[7] with the choice of a prototype catalytic reaction for initial survey studies[7,8] (hydrogenations; relatively simple, well studied reactions, yet still of scientific and technological importance).[10] The discovery of **1** demanded *concurrent* efforts in three areas: in polyoxoanion synthesis and characterization (often the slow and most difficult step),[1] in catalysis (initial survey experiments),[7,8] and in kinetic and mechanistic studies (reported elsewhere)[4] probing the central issue of whether or not polyoxoanion–iridium bonding remains intact during catalysis.

$$(Bu_4N)_9P_2W_{15}Nb_3O_{62} + [(1,5\text{-}COD)Ir(CH_3CN)_2]BF_4 \xrightarrow[\substack{3)\ 2\ EtOAc\ Reppt.\\ (-4\ Bu_4NBF_4)}]{\substack{1)\ CH_3CN\\ 2)\ 3\ NaBF_4}} (Bu_4N)_5Na_3[(1,5\text{-}COD)Ir\cdot P_2W_{15}Nb_3O_{62}] \quad (1)$$

1

The choice of the metal–ligand combination Ir(1,5-COD)$^+$ was based on the literature,[11] and our synthesis of $(Bu_4N)_9P_2W_{15}Nb_3O_{62}$ has been previously described.[1d,h] The synthesis (eq 1) and subsequent storage of **1** require strict O_2-free conditions (a ≤2 ppm O_2 drybox).[12] The key to isolating **1** as a pure solid is our recent method[13] employing mixed Bu_4N^+/Na^+ salts[13b] and at least two reprecipitations from paper-filtered, homogeneous CH_3CN solution using EtOAc (Bu_4NBF_4 is very soluble in EtOAc and thus is removed by this process). Analytically pure **1** is obtained as a bright yellow, very air-sensitive powder in 69% (4.2 g) yield (anal. all elements; total 99.4%).[14a] Ultracentrifugation molecular weight measurements[2d] (1×10^{-5} M **1**, 0.1 M Bu_4NPF_6/CH_3CN) show that **1** is an unaggregated monomer under these conditions [Calc for **1**, $(Bu_4N)_5Na_3[(1,5\text{-}COD)Ir\cdot P_2W_{15}Nb_3O_{62}]$, M_r = 5670; found, $\bar{M}_r$ (weight-average molecular weight) = 6000 ± 600 (Figure A, supplementary material)].

---

(8) (a) Studies of $(Bu_4N)_4Na_2[(1,5\text{-}COD)Ir\cdot SiW_9Nb_3O_{40}]$ and $(Bu_4N)_5Na_3[(COD)Rh\cdot P_2W_{15}Nb_3O_{62}]$ will be reported elsewhere. Survey work involving H_2 prereduction of oxidized forms of the all Bu_4N^+ salts of these and other catalyst precursors is also available.[8b] (b) Edlund, D. J. Ph.D. Dissertation, University of Oregon, 1987. U.S. Patent Application US 88 00609, filed Feb 17, 1987.

(9) (a) Halpern, J.; Okamoto, T.; Zakharier, A. *J. Mol. Catal.* **1976**, *2*, 65. Halpern, J. *Inorg. Chim. Acta* **1981**, *50*, 11. (b) Collman, J. P.; Hegedus, L. S.; Norton, J. R.; Finke, R. G. *Principles and Applications of Organotransition Metal Chemistry*; University Science: Mill Valley, CA, 1987; Chapter 10.

(10) Efforts at more challenging reactions, including oxygenations and alkane activation and selective functionalizations, are in progress.

(11) (a) Green, M.; Kuc, T. A.; Taylor, S. H. *J. Chem. Soc. A* **1971**, 2334. (b) Schrock, R. R.; Osborne, J. A. *J. Am. Chem. Soc.* **1971**, *93*, 3089. (c) *Idem.*, p 2397. (d) Synthesis used for $[Ir(1,5\text{-}COD)Cl]_2$: Crabtree, R. H.; Quirk, J. M.; Felkin, H.; Fillebeen,-Kahn, T. *Synth. React. Inorg. Met.-Org. Chem.* **1982**, *12*, 407. Herdê, J. L.; Lambert, J. C.; Senoff, C. V. *Inorg. Synth.* **1974**, *15*, 18. (e) As the work described herein has proceeded,[7,8] valuable reports by Klemperer, Day, and co-workers have appeared describing M(1,5-COD)$^+$ (M = Rh, Ir) covalently attached to the smaller, well-characterized polyoxoanions $P_3O_9^{3-}$ and $Nb_2W_4O_{19}^{4-}$ and in a variety of M to polyoxoanion stoichiometries and bonding geometries.[12c–e]

(12) (a) Polyoxoanion-supported Ir(COD)$^+$ is much more air sensitive than $[Ir(COD)Cl]_2$. We anticipate that the Ir(I) to Ir(II) or Ir(III) oxidation potential in **1** is markedly shifted to more positive, thermodynamically more favorable potentials due to iridium's proximity and inner-sphere attachment to the polyanionic polyoxoanions. Electrochemical studies aimed at comfirming and quantifying this effect are planned. (b) The O_2 sensitivity of **1** presages its potentially rich dioxygen and oxygen atom-transfer chemistry.[4c,12d,e] (c) Klemperer, Day, and Main[12d] have crystallographically characterized the 5-coordinate, C_s symmetry, yellow-green Ir(I) complex $(Bu_4N)_2[(COD)Ir\cdot P_3O_9]$ as well as the 4-coordinate, orange Ir(I) complex $(Bu_4N)_3\{[(COD)Ir]_5\cdot[Nb_2W_4O_{19}]_2\}$ and the yellow complex $(Bu_4N)_5\{[(COD)Ir]_2H[Nb_2W_4O_{19}]_2\}$: Day, V. W.; Klemperer, W. G.; Main, D. J. *Inorg. Chem.*, in press. The ^1H NMR spectrum (300 MHz, CD_2Cl_2, 22 °C) of $(Bu_4N)_2[(COD)Ir\cdot P_3O_9]$ consists of *three* lines, δ 3.6 (m, CH), 2.1 (m, CH_2), and 1.2 (q, CH_2) and has been interpreted in terms of Berry pseudorotation fluxionality at Ir(I). (d) Main, D. J. Ph.D. Thesis, University of Illinois, May 1987. (e) Day, V. W.; Klemperer, W. G.; Lockledge, S. P.; Main, D. J. *J. Am. Chem. Soc.* **1990**, *112*, 2031.

(13) (a) Finke, R. G.; Droege, M. W.; Nomiya, K.; Green, C. A. *Inorg. Synth.* **1989**, *27*, in press (describing the synthesis of $(Bu_4N)_3(Na)_2[(C_5Me_5)Rh\cdot SiW_9Nb_3O_{40}]$). (b) No suitable purification process has been found that provides the all Bu_4N^+ analogue[7b,8b] of **1** in ≥10% yield of *pure* material; hence, the development of the mixed Bu_4N/Na salt isolation method[13a] proved essential to this work.

(14) (a) Calculated for $C_{88}H_{192}N_5Na_3IrP_2W_{15}Nb_3O_{62}$: C, 18.63; H, 3.41; N, 1.23; Na, 1.22; Ir, 3.39; P, 1.09; W, 48.6; Nb, 4.91; O, 17.5. Found (Mikroanalytisches Labor Pascher, Remagen, FGR): C, 18.95; H, 3.54; N, 1.49; Na, 1.43; Ir, 2.74; P, 1.09; W, 48.4; Nb, 4.80; O, 17.0 (total, 99.4). (b) Ion-pairing effects in *aqueous* polyoxometalate chemistry have been reported: Clare, B. W.; Kepert, D. L.; Watts, D. W. *J. Chem. Soc., Dalton Trans.* **1973**, 2481. Druskovich, D. M.; Kepert, D. L. *J. Chem. Soc., Dalton Trans.* **1975**, 947. Druskovich, D. M.; Kepert, D. L. *Aust. J. Chem.* **1975**, *28*, 2365–2372. Kepert, D. L.; Kyle, J. H. *J. Chem. Soc., Dalton Trans.* **1978**, 137. In organic solvents, Na^+ to $P_2W_{15}Nb_3O_{62}^{9-}$ ion-pairing effects are reminescent of the multiple sites of H^+ attachment, and slow proton mobility (tautomerism), observed in the $SiW_9V_3O_{40}^{7-}$ system[2b] in organic solvents. (c) In an initial control experiment, **1** was found to be thermally stable at 60 °C under N_2 for at least 24 h as demonstrated by ^{31}P (0.05 M in CH_3CN) and ^{183}W NMR spectroscopy (0.1 M in DMSO)].

To date, all attempts to obtain crystals of **1** suitable for an X-ray diffraction structural investigation have failed. However, we were able to obtain the structure shown in Figure 1A[1h] for the $(Na^+)_9$ salt of the parent $P_2W_{15}Nb_3O_{62}^{9-}$ polyoxoanion in **1**. Not shown in Figure 1A are the 2.3–2.5-Å $Na^+\cdots P_2W_{15}Nb_3O_{62}^{9-}$ solid-state, "ion-pairing" interactions present in $Na_9P_2W_{15}Nb_3O_{62}$. Such ion-pairing[14b] *persists in solution*, causing the extra peaks or line broadening observed in the solution ^{31}P NMR spectra of **1**, for example (vide infra).

Further characterization of **1** relied heavily on the extremely valuable ^{183}W and ^{31}P NMR spectroscopic probes in $P_2W_{15}Nb_3O_{62}^{9-}$. (Initial NMR control experiments[14c,15a] demonstrate that the NMR spectra of air-sensitive **1**, obtained in sealable J. Young NMR tubes,[15a] are free from artifacts due to oxidation by adventitious O_2.) The ^{31}P NMR spectrum of **1** exhibits primarily two equal integrated-intensity lines (Figure C, supplementary material), but the downfield, $\delta = -9.0$ ppm resonance (the PO_4 closest to the Nb_3O_6 support site, Figure 1) is flanked by two smaller peaks at −7.9 and −10.0 ppm. Suspecting $Na^+\cdots[P_2W_{15}Nb_3O_{62}]^{9-}$ ion pairing as the source of these extra peaks, 3 equiv of the cryptand Kryptofix 2.2.2. (4,7,13,16,21,24-hexaoxa-1,10-diazabicyclo[8.8.8]hexacosane) was added to the NMR tube in the drybox, and the ^{31}P NMR spectrum was remeasured. The smaller peaks collapse into the center, −9.0 ppm resonance, and the half-widths of the ^{31}P resonances are reduced 4–5-fold down to their normal, $\Delta\nu_{1/2} = 1$–2 Hz, values (Figure D, supplementary material). These ^{31}P results (Figures C and D, supplementary material) demonstrate that ≥95% of a single isomer of **1** has been achieved, an unprecedented result for a polyoxoanion presenting multiple support sites (multiple possible regioisomers) to an organometallic monocation like $(1,5\text{-COD})Ir^+$. These NMR results also demonstrate the anticipated,[1d] but previously undocumented,[14c] existence of ion-pairing effects in nonaqueous polyoxometalate chemistry.

The ^{183}W NMR spectra of **1** in DMSO without and with Kryptofix 2.2.2. are shown in Figure 2A,B, respectively. Both spectra show primarily 3 peaks indicating that **1** has effective C_{3v} symmetry[15b] on the ^{183}W NMR time scale (although the local symmetry at Ir is C_s),[15b] but the signal to noise (S/N) is increased 2-fold by the addition of Kryptofix (Figure 2A, S/N = 12/1 for 10000 scans; Figure 2B (added Kryptofix), S/N = 25/1 for 10000 scans). The increased S/N is readily explained[1b,e] by the removal of the $Na^+\cdots P_2W_{15}Nb_3O_{62}^{9-}$ ion pairing and thus the increased concentration of a single form of **1**. However, even in the presence of Kryptofix 2.2.2. the ^{183}W NMR resonances are roughly 2–3-fold broader than normal[1a,c,d] ($\Delta\nu_{1/2} = 11$–14 Hz for 0.09 M **1** in DMSO-d_6) due, presumably, to the fluxionality at Ir discussed below.

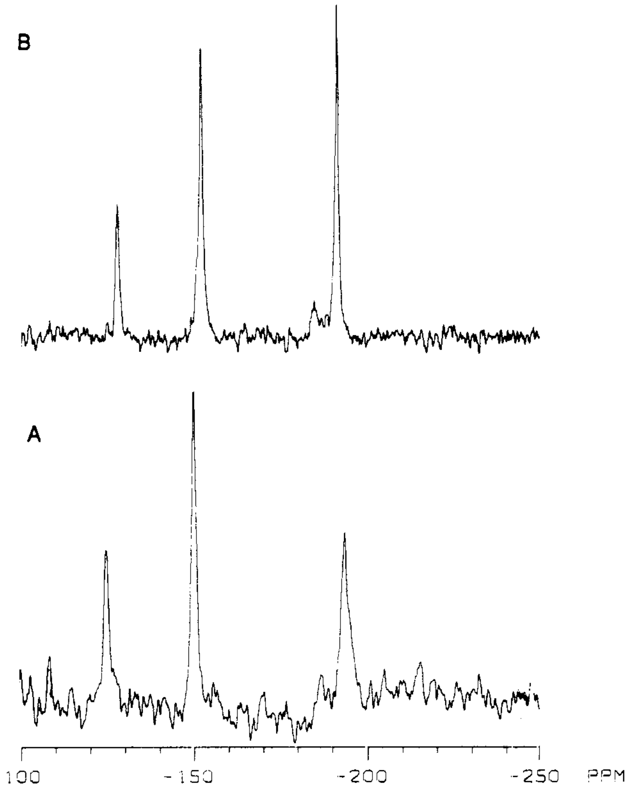

Figure 2. 1:2:2 relative intensity three-line ^{183}W NMR spectra (15.041 MHz, 30 °C, DMSO-d_6, sealed J. Young NMR tube[15a]). (A) Spectrum of 0.09 M **1** after 10000 scans collected over 5 h, S/N = 12/1 {δ (no. of W) [$\Delta\nu_{1/2}$]}: −125.0 (3) [14.9 ± 1.0 Hz], −150.3 (6) [13.7 ± 0.7 Hz], −194.0 (6) [25.5 ± 1.5 Hz]. (B) Spectrum of 0.09 M **1** with 3 equiv of Kryptofix 2.2.2. added after 10000 scans collected over 5 h, S/N = 25 ± 1 {δ (no. of W) [$\Delta\nu_{1/2}$]}: −128.1 (3) [12.0 ± 0.3 Hz], −152.2 (6) [−13.9 ± 0.2 Hz], −191.4 (6) [11.1 ± 0.2 Hz]. The ^{183}W samples were referenced to 2 M Na_2WO_4 in 1:1 D_2O/H_2O by the external substitution method.

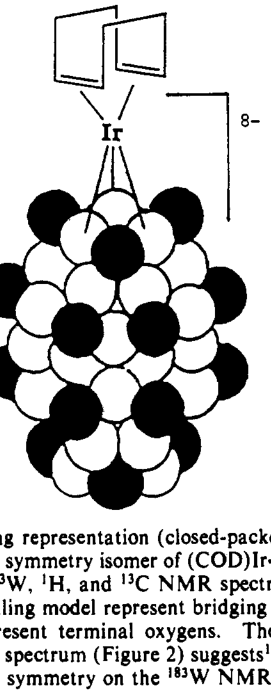

Figure 3. Space-filling representation (closed-packed oxygens) of one 5-coordinate, static C_s symmetry isomer of $(COD)Ir\cdot P_2W_{15}Nb_3O_{62}^{8-}$, as determined by ^{31}P, ^{183}W, ^1H, and ^{13}C NMR spectroscopy. The open circles in the space-filling model represent bridging oxygens, while the darkened circles represent terminal oxygens. The observation of a three-line ^{183}W NMR spectrum (Figure 2) suggests[15b] fluxionality at Ir to attain effective C_{3v} symmetry on the ^{183}W NMR time scale.

The presence of six broad ^1H NMR 1,5-COD ligand resonances[15c] (integrating to two hydrogens each) for **1** requires local C_s symmetry and strongly suggests that Ir is 5-coordinate[15d,e] (i.e. bonded to three polyoxoanion surface oxygens, probably by two normal and one longer Ir–O bond as found in $(Bu_4N)_2[(COD)Ir\cdot P_3O_9]$).[12c] Adding 3 equiv of Kryptofix 2.2.2. has little effect

---

[15] (a) All NMR spectra reported herein were obtained by using sealed J. Young Teflon-valve NMR tubes (5-, 10-, and 12-mm o.d. for ^1H, ^{183}W, and ^{31}P NMR spectra, respectively; Wilmad Glass Co.) exposed to the atmosphere for ≤1.5 h (^1H and ^{31}P) or ≤48 h (^{183}W) while the spectra where recorded. Two types of control experiments confirmed that these NMR tubes, prepared and then sealed in the drybox, excluded O_2 for at least 1 week (details are available as supplementary material). (b) This argument, which assumes that any non-C_{3v} symmetry isomers of **1** would be detected by the ^{183}W NMR spectroscopy, is supported by the fact that even Na^+ ion-pairing is detectable as excess line width in the ^{183}W NMR spectrum. Alternatively, the true symmetry of **1** may be C_s symmetry as detected by ^1H NMR[15d] (see Figure 3), with the ^{183}W NMR simply proving insensitive to this C_s symmetry. (c) The ^1H NMR data for **1** is available as supplementary material. (d) Four- and five-coordinate, static C_s symmetry isomers of **1**, where the $(1,5\text{-COD})Ir^+$ is attached, respectively, to two or three bridging Nb–O–Nb oxygens of the Nb_3O_9 "cap" in $P_2W_{15}Nb_3O_{62}^{9-}$, each would have six magnetically nonequivalent COD hydrogens. To achieve the effective C_{3v} symmetry suggested[15b] by the ^{183}W NMR spectrum (Figure 3), fluxionality in **1** must occur about the C_3 rotational axis of $P_2W_{15}Nb_3O_{62}^{9-}$ (see Figure 1A). Such fluxionality should produce three ^1H NMR peaks for the CN = 4 isomer of **1** described above, and three to six peaks for the CN = 5 isomer (three peaks are seen for $(Bu_4N)_2[(COD)Ir\cdot P_3O_9]$).[12d] Since six peaks are observed,[15c] the ^1H NMR data strongly suggest the presence of 5-coordinate, C_s symmetry, fluxional $(1,5\text{-COD})Ir^+$ in **1**. (e) In the ^{183}W NMR spectrum, the line widths roughly double due to the increased solution viscosity in going from a 0.07 to 0.13 M solution of **1** in CH_3CN at 21 °C.

on the ^{1}H NMR line widths. Because d^8, 5-coordinate Ir(I) is well-known to be highly fluxional,[16] we presently assign the majority of the ^{1}H NMR line broadening (and the residual ^{183}W NMR line broadening) to such fluxionality, and variable-temperature ^{1}H NMR studies are in progress. Any detailed description of the fluxionality in **1** must take note of the fact that a (1,5-COD)Ir$^+$ fragment of inherent C_2 symmetry has been supported atop a $P_2W_{15}Nb_3O_{62}{}^{9-}$ polyoxoanion of inherent C_3 symmetry.

These NMR results demonstrate that the C_{3v} symmetry designed into $P_2W_{15}Nb_3O_{62}{}^{9-}$ (via triniobium substitution)[1d] leads to the unprecedented ability[1e,6] to form predominantly one type of support-site regioisomer, (1,5-COD)Ir$^+$ attached to the Nb_3O_9 "cap" in **1** with effective C_{3v} symmetry (Figure 3). The ability of $P_2W_{15}Nb_3O_{62}{}^{9-}$ to form 1:1 metal/polyoxoanion complexes that do not aggregate is a further, highly desirable, and distinguishing feature of **1**.

The ability of **1** to serve as an effective catalyst precursor, and initial kinetic and mechanistic studies of the resultant high-activity catalyst, are described in the following communication.[4]

Acknowledgment. We thank the reviewers for their helpful comments. Support from NSF Grant CHE-831345 and from a cooperative academic–industrial grant from Catalytica Associates is gratefully acknowledged.

Supplementary Material Available: Figures A and B (ln *A* vs r^2 MW plots for **1** and the catalyst, respectively), Figures C and D (^{31}P NMR spectra of **1** with and without Kryptofix 2.2.2. in DMSO), Figures E and F (^{31}P NMR spectra of **1** with and without Kryptofix 2.2.2. in CH_3CN, showing the more pronounced ion-pairing effects in that solvent in comparison to DMSO), text containing details of the control experiments ruling out O_2 contamination during the NMR studies of **1** in J. Young NMR tubes, and text containing the ^{1}H NMR data for **1** (6 pages). Ordering information is given on any current masthead page.

---

(16) (a) Shapley, J. R.; Osborn, J. A. *Acc. Chem. Res.* **1973**, *6*, 305 and references therein. (b) Churchill, M. R.; Lin, K.-K. G. *J. Am. Chem. Soc.* **1974**, *96*, 76 and earlier papers cited therein in this series. (c) Rossi, A. R.; Hoffman, R. *Inorg. Chem.* **1975**, *14*, 365. (d) Adams, H.; Bailey, N. A.; Mann, B. E.; Taylor, B. F.; White, C.; Yavari, P. *J. Chem. Soc., Dalton Trans.* **1987**, 1947. (e) Mestroni, G.; Camus, A.; Zassinovich, G. *J. Organomet. Chem.* **1974**, *73*, 119 and references 1–3 therein.

(17) Current address: Department of Chemistry, Faculty of Science, Kanagawa University, Hiratsuka 259-12, Kanagawa, Japan.

(18) Current address: Catalysis Research Center, Hokkaido University, Sapporo, Japan.

Department of Chemistry
University of Oregon
Eugene, Oregon 97403

Richard G. Finke*
David K. Lyon
Kenji Nomiya[17]
Sandip Sur
Noritaka Mizuno[18]

Received November 30, 1989

Polyoxoanions as Soluble Metal Oxide Analogues. 6.[1] Catalytic Activity and Initial Kinetic and Mechanistic Studies of Polyoxoanion-Supported, Atomically Dispersed Iridium(I), $(1,5\text{-COD})Ir{\cdot}P_2W_{15}Nb_3O_{62}{}^{8-}$

In the preceding communication[1] we described the synthesis and characterization of the polyoxoanion-supported Ir(I) precatalyst $(Bu_4N)_5Na_3[(1,5\text{-COD})Ir{\cdot}P_2W_{15}Nb_3O_{62}]$ (**1**). Herein we (a) demonstrate that **1** leads to an active and long-lived catalyst in a prototypical catalytic reaction, olefin hydrogenation and (b) report initial kinetic and mechanistic data which provide evidence that the actual catalyst derived from **1** is indeed polyoxoanion-supported.

Scheme I

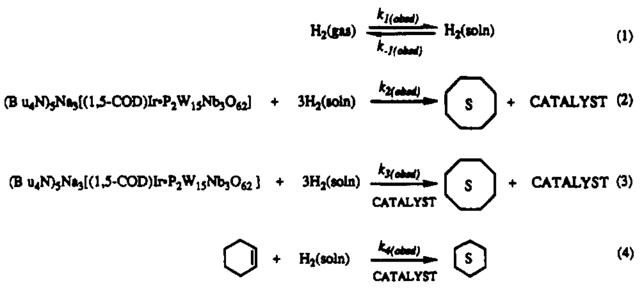

In the presence of 40 psig H_2 and 1.65 M purified[2] cyclohexene in acetone at 22.0 ± 0.1 °C, seven independent preparations of **1** (0.0012 M) evolve *reproducibly* into a highly active, yellow, clear and thus *apparently* homogeneous hydrogenation catalyst (eq 1 and Figure 1).[3] The catalyst evolves from **1** during a reproducible 1.2 ± 0.5 h induction period and with the production of 1.00 ± 0.08 equiv of cyclooctane but without producing any visible or insoluble Ir(0).[4] Separate H_2-uptake experiments (13 mM **1**, acetone, 22 °C, 500 Torr H_2, *no olefin*) show that **1** consumes 3.0 equiv of H_2 over 15 h (eq 1a) to yield 1.0 equiv of cyclooctane and a species showing a ^{1}H NMR hydride resonance at −14.5 ppm. The H_2-pressure-loss kinetic data (Figure 1, squares with center dots) can be curve-fit (Figure 1, solid line) by the four-step *minimum kinetic model*[5] shown in Scheme I, eqs 1–4.

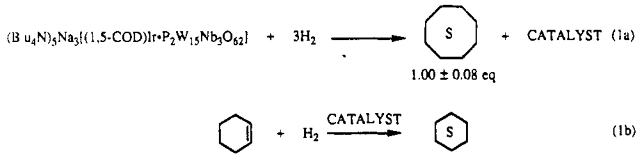

---

(1) Part 5: Finke, R. G.; Lyon, D. K.; Nomiya, K.; Sur, S.; Mizuno, N. *Inorg. Chem.*, preceding communication in this issue. Non-SI units employed herein: 1 psig = 0.068 atm = 51.68 Torr = 6.89 × 10^3 Pa.

(2) Cyclohexene (Baker) was distilled from Na under dry N_2 and stored in the drybox. Acetone (Burdick and Jackson) was distilled from K_2CO_3 under dry N_2 and stored in the drybox. Both liquids were dispensed and stored in glassware that had been dried at 250 °C and cooled under a dry nitrogen flow. H_2 (Air Products) was purified by passage through an indicating moisture trap and disposable cartridge O_2 trap (Scott).

(3) Details of the catalytic hydrogenations are available as supplementary material.

(4) No Ir(0) metal precipitates visible to the naked eye appear in the hydrogenation experiments described in the text. If the experiment is run at higher catalyst (≥1 mM) or olefin (≥1 M) concentrations, a precipitate is formed at the end of the experiment that is 3–4 times less soluble than **1** and that we are attempting to characterize (the precipitate, which is both acetone and acetonitrile soluble, is not $[Ir(0)]_n$).

(5) (a) The numerical integration curve-fitting[5b] presented in Figure 1 was performed with the GEAR[5c] and the GEAR Iterator[5d] (GIT) programs. (b) McKinney, R. J.; Weigert, F. J. Quantum Chemistry Program Exchange, Program No. QCMP022. (c) Stabler, R. N.; Chesick, J. *Int. J. Kinet.* **1978**, *10*, 461. (d) Weigert, F. J. *Comput. Chem.* **1987**, *11*, 273. (e) As incorporated herein, the correct approach[5d] (Occam's razor) toward such numerical integration curve-fitting is to use the minimum number of steps but also to be sure that only *elementary steps* are used in any final kinetic model. Step 4 ($k_{4,\text{obsd}}$) cannot be an elementary step since it goes from a first-order to a zero-order dependence (i.e. exhibits saturation kinetics)[7d] in both H_2 and cyclohexene at ca. ≥30 psig and ca. ≥1.5 M, respectively. Steps 2 and 3 are unlikely to be elementary steps since they are greater than termolecular. [In fact, the stoichiometry-based steps 2 and 3 had to be approximated in the actual modeling by incorporating only 2 and 1 equiv of H_2, respectively, since the program[5a–d] is (correctly) limited to termolecular (elementary) steps.] Hence, we have not reported the physically meaningless $k_{2,\text{obsd}}$, $k_{3,\text{obsd}}$, and $k_{4,\text{obsd}}$ values corresponding to eqs 2–4 (Scheme I). However, some type of autocatalytic step (e.g. step 3) is essential even in a seven-step mechanism,[7d] our best fit to date. Moreover, the formation of cyclooctane (and not the anticipated cyclooctene)[5h] can be explained by such a step. (f) Under the conditions of the kinetic studies (1.65 M cyclohexene, 0.0012 M **1**), measurable H_2 consumption (≥0.02 psi) occurs only via eq 4. (g) The solubility data for H_2 in acetone is from: *The Matheson Unabridged Gas Book*; *Hydrogen*; Matheson: East Rutherford, NJ, 1974. (h) Green, M.; Kuc, T. A.; Taylor, S. H. *J. Chem. Soc., Chem. Commun.* **1970**, 1553. Schrock, R. R.; Osborn, J. A. *J. Am. Chem. Soc.* **1971**, *93*, 3089.

0020-1669/90/1329-1787$02.50/0